Optics Communications 407 (2018) 127–131

Contents lists available at ScienceDirect

Optics Communications

journal homepage: www.elsevier.com/locate/optcom

Theoretical investigation of the isolated attosecond pulse generation by restraining the spatial distribution of high-order harmonic emission

Chang-Long Xia, Qi-Ying Liu, Xiang-Yang Miao *

College of Physics and Information Engineering, Shanxi Normal University, Linfen 041004, , People's Republic of China

ARTICLE INFO

Keywords:
Isolated attosecond pulse
High-order harmonic generation
Chirped laser pulse

ABSTRACT

Isolated attosecond pulse (IAP) generation is theoretically investigated by using a few-cycle laser pulse from a two-dimensional model of hydrogen molecular ion. The harmonic spectra from two nuclei of hydrogen molecular ion lead to interference. We investigate the spatial distribution in harmonic generation and propose a scheme to restrain the harmonic generation from the nucleus along the positive-x direction, and thus the interference is weaken in spatial. By using a few-cycle 800 nm chirped laser pulse, the harmonics are mainly generated from the nucleus along negative-x direction in the region of 130th to 230th order. The harmonic spectra are smooth and are mainly contributed by the short quantum path near the cutoff region and IAP with a duration of 97 as is generated. The semiclassical of three-step model is also used to illustrate the physical mechanism.

1. Introduction

High-order harmonic generation (HHG) from atoms or molecules has been a hot topic in past few decades because of its promising application [1–5]. One of the most attractive application is to obtain isolated attosecond pulse (IAP) [6–9] and IAP can be used to probe ultrafast dynamics of electron in atoms or molecules [10,11]. The high-order harmonic spectrum has a plateau structure and can be explained by semiclassical three step model [12]: Firstly, an electron is ionized as a quantum process. Secondly, the electron is accelerated as a classical particle. Finally, the accelerated electron has a probability to be driven back to the parent ion and emit a high energy photon. This model gives a clear physical mechanism of HHG and only the ionized electron recombining with the parent ion contribute to HHG. In particular, the ionized electron can recombine with two or more nuclei in molecule or cluster system. This may affect the spatial distribution of HHG and the interference of quantum path. The spatial properties of electron have been investigated in both experiment and theory [13–16]. However, the HHG generating from which nucleus is seldom concerned [17,18]. In this work, we investigate the IAP generation by restraining spatial distribution in HHG from a model of $H_2{}^+$ molecule.

IAP generation which can be obtained by superposing a bandwidth of HHG spectrum has been investigated widely [19–21]. A series of schemes have been proposed to obtain IAP, such as few-cycle scheme [7,22], two-color scheme [23–25], polarization gating [26–28] and so on. Salières et al. [29] found that focusing conditions and chirped driving fields can be used to control the harmonic spectrum. Chirped laser pulse and its combination schemes are investigated to generate IAP, control or broaden the harmonic spectrum [30–32]. However, the spatial distribution of HHG from chirped pulse has seldom investigated. As a simple model of two nuclei system, HHG from Hydrogen molecular ion has been investigated a lot [33–35]. Recently, Zhang et al. [36] investigated the spatial distribution in HHG from the model of $H_2{}^+$ molecule, but the electron is only in one dimension. In this paper, two-dimensional Schrödinger equation is solved to investigate IAP generation. A chirped pulse is used to restrain the spatial distribution of HHG and IAP can be generated by eliminating the interference of HHG from two nuclei. Semiclassical of three-step model and Morlet wavelet analysis are used to illustrate the physical mechanism.

2. Theoretical model and numerical method

A model ion of $H_2{}^+$ irradiated with an intense laser pulse is investigated by numerically solving time-dependent Schrödinger equation. With Born–Oppenheimer Approximation (BOA), the two-dimensional Schrödinger equation can be written in atomic units as

$$i\frac{\partial\Psi(x,y,t)}{\partial t}=\left[\frac{p_x^2+p_y^2}{2}+V(x,y)+xE_x(t)\right]\Psi(x,y,t). \quad (1)$$

* Corresponding author.
E-mail addresses: xiachl2008@163.com (C.-L. Xia), sxxymiao@126.com (X.-Y. Miao).

http://dx.doi.org/10.1016/j.optcom.2017.09.030
Received 22 June 2017; Received in revised form 4 September 2017; Accepted 7 September 2017
Available online 19 September 2017
0030-4018/

The soft-Coulomb potential is used in our simulation,

$$V(x, y) = \frac{-1}{\sqrt{(x - R/2)^2 + y^2 + a}} + \frac{-1}{\sqrt{(x + R/2)^2 + y^2 + a}}, \tag{2}$$

where R is the distance of the two nuclei and a is the soft-core parameter. We set $a = 0.61$ and $R = 7$ a.u. in the calculation. The energy of ground electronic state is 0.519 a.u. (including the 1/R nuclear repulsion) which is corresponding the model of $H_2{}^+$. A chirped laser pulse with Gaussian envelope is chosen as $E_x(t) = E_0 f(t)\cos[\omega_0 t + \delta(t) + \varphi]$ and its polarization direction is along x axis. Where $f(t) = exp(-4ln2t^2/\tau_0^2)$ is the laser envelope and τ_0 is the full width at half maximum (FWHM). $\delta(t) = \alpha t^2 + \beta t^3$ and the parameters α and β are used to control the chirp form. φ is the carrier envelope phase (CEP). The Eq. (1) is solved by the well-known second-order split-operator method [37,38]. Once we obtain the wave function, the time-dependent dipole acceleration can be given by the Ehrenfest theorem,

$$a_x(t) = \langle \Psi(x, y, t)| - \frac{\partial V(x, y)}{\partial x} - E_x(t)|\Psi(x, y, t)\rangle. \tag{3}$$

The relative intensity of the HHG spectrum is proportional to

$$S(\omega) \sim \left| \int exp(-i\omega t) a_x(t) dt \right|^2. \tag{4}$$

To further investigate the spatial distribution in HHG, we calculate the dipole acceleration distribution as a function of x coordinate due to the nuclei are in x axle [17,18],

$$d_A(x, t) = \int_{-\infty}^{+\infty} \Psi^*(x, y, t)[-\frac{\partial V(x, y)}{\partial x} - E_x(t)]\Psi(x, y, t) dy. \tag{5}$$

The cutoff position of HHG can be well explained by the semiclassical three-step model. In our calculation, the polarization direction of the laser pulse is along x axis, so we simulate the process by one-dimensional model. After the electron ionized by tunnel effect, it is accelerated as a classical particle:

$$\ddot{x}(t) = -E_x(t). \tag{6}$$

Assume the initial velocity of the ionized electron is zero at t_i and the initial position x_0 is at the nucleus of A or B. The nucleus at $-R/2$ or $R/2$ is called A or B for short in this paper. We have

$$\dot{x}(t) = \int_{t_i}^{t} -E_x(t) dt, \tag{7}$$

and

$$x(t) = \int_{t_i}^{t} \dot{x}(t) dt + x_0. \tag{8}$$

The electron has a probability to be driven back to the nucleus A or B and then emits a high energy photon at t_e. The time t_e can be obtained by solving the equation

$$x(t) = \int_{t_i}^{t_e} \dot{x}(t) dt + x_0 = \pm R/2. \tag{9}$$

$x(t_e)$ equates $-R/2$ ($R/2$) is corresponding to the recombination to nucleus A (B). The kinetic energy can be obtained by $E_k = 1/2\dot{x}^2(t_e)$.

3. Results and discussion

A few-cycle laser pulse with the FWHM of 5 fs and the wavelength of 800 nm is used in our calculation. First, we investigate the harmonic spectrum with different chirp parameters, and the intensity is set to 1×10^{15} W/cm^2. As shown by solid black in Fig. 1, the plateau of harmonic spectrum is around with modulations and the cutoff is about 140th order for the case of chirped free pulse. As shown by dashed red line and dotted green line, the cutoff of the spectrum increase to 150th order and 155th order for the case of $\beta = 0$ and $\beta = -2 \times 10^{-7}$, the parameter α is set to 2×10^{-4} and the CEP is 0. The intensity of HHG is stronger near the cutoff region for the case $\beta = -2 \times 10^{-7}$ than for the

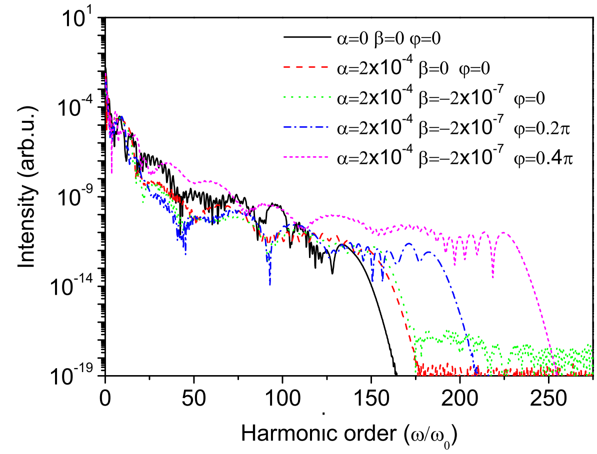

Fig. 1. HHG from different parameters of laser pulse. Solid black line shows for the case of $\alpha = \beta = \varphi = 0$. Dashed red line shows for the case of $\alpha = 2 \times 10^{-4}$ and $\beta = \varphi = 0$. The other lines show for the case of $\alpha = 2 \times 10^{-4}$, $\beta = -2 \times 10^{-7}$ with different CEPs. For the case of $\varphi = 0$, $\varphi = 0.2\pi$ and $\varphi = 0.4\pi$ are shown by dotted green line, dash-dotted blue line and short-dashed magenta line, respectively. (For interpretation of the references to color in this figure legend, the reader is referred to the web version of this article.)

case $\beta = 0$. As we all know that the CEP is very important in few-cycle scheme, we investigate the HHG with different CEPs. The results are shown by dash-dotted blue line and short-dashed magenta line for the case of $\varphi = 0.2\pi$ and $\varphi = 0.4\pi$. The cutoff of the spectrum is extended to 190th order and 230th order respectively. The intensity of HHG for the case $\varphi = 0.4\pi$ is one order higher than the other cases. We investigate the spatial distribution of HHG for further discussion.

The spatial distribution in HHG can be demonstrated by the modulus square of the Fourier transform of Eq. (5). Fig. 2(a) shows the spatial distribution in HHG for the case of chirped free scheme. The intensity of HHG from the position $x = 0, \pm R/2$ is weak, which is agreement with the results demonstrated in Ref. [17,18]. HHG from the nucleus B is as strong as that from the nucleus A in the plateau region, but the HHG is mainly from the nucleus A near the cutoff region, *e.g.*, from 115th to 140th order. Fig. 2(b), (c) and (d) show the spatial distributions in HHG with different CEPs for the case $\alpha = 2\times10^{-4}$ and $\beta = -2\times10^{-7}$. As shown in Fig. 2(b) and Fig. 2(c), both nuclei contribute to the HHG for the case $\varphi = 0$ and $\varphi = 0.2\pi$ and the intensity from the nucleus B is a litter weaker than from nucleus A in the plateau region. The intensities for those two cases are much weaker than as shown in Fig. 2(a) below 100th order. This is corresponding to the intensities of harmonic spectra shown in Fig. 1, the intensity of HHG shown by solid black line is stronger than that shown by the dotted green line and dash-dotted blue line in this region. For the case of $\varphi = 0.4\pi$, both nuclei contribute to the HHG as shown in Fig. 2(d). The contribution from two nuclei is comparable in the low order region. However, the contribution from the nucleus A is greater than the other in the region from 130th to 230th order. The interference of HHG from the two nuclei turns weak, so there is little modulation in the region of 130th order to 230th order. Those characters corresponds to the structure of HHG spectrum shown in Fig. 1.

Next, to explain the spatial distribution of Fig. 2, we calculate the kinetic energy of the electron by classical method. As shown in Fig. 3(a) and Fig. 3(c), for the case of the initial position of the electron from the nucleus A, *i.e.*, $x_0 = -R/2$, the kinetic energy is shown with triangle. For the case $x_0 = R/2$, circle or square is used. The hollow symbols show the kinetic energy of ionization time and the solid symbols show the kinetic energy of recombination time. For the case of chirped free scheme, three returning kinetic energy peaks are marked with P_{e1}, P_{e2} and P_{e3}, and the corresponding peaks of ionization time are marked with P_{i1}, P_{i2} and P_{i3}, as shown in Fig. 3(a). Fig. 3(b) shows the electronic wave packet density by calculating the square modulus of the wave function. The electron is distributing near both of the nuclei before 3.0 o.c., which is include the